

ORIGINAL ARTICLE

Physical and Mechanical Properties of Chitosan Bioplastics with Ramie Fiber Concentration Variations

U. L. Jamilah¹, Sujito¹, N. Hidayatillah¹, and E. Hidayah²¹ Department of Physics, Faculty of Mathematics and Natural Sciences, University of Jember, Jember, Indonesia² Faculty of Tarbiyah and Education, Universitas KH. Mukhtar Syafaat, Banyuwangi, Indonesia

ABSTRACT – Bioplastics are biodegradable materials derived from natural polymers such as starch, cellulose, lignin, or chitosan and are considered sustainable alternatives to conventional plastics. In this study, chitosan-based bioplastics were prepared using chitosan extracted from fish scales and reinforced with alkali-treated ramie fibers. Chitosan was dissolved in 1% acetic acid at 50 °C for 4 h, followed by the addition of 5% citric acid and ramie fibers at various contents (15%, 20%, 25%, and 30% relative to chitosan mass), and stirred for an additional hour. The resulting bioplastics were characterized for tensile strength, elastic modulus, water absorption, and surface morphology using SEM. The results indicate that ramie fiber content significantly influences the mechanical and physical properties of the bioplastics. Increasing the fiber content generally enhances tensile strength and reduces water absorption; however, excessive fiber loading can lead to performance deterioration. The optimum formulation was achieved at 25% ramie fiber, exhibiting a tensile strength of 39.60 MPa, an elastic modulus of 43.35 MPa, and a reduction in water absorption of approximately 43% compared to fiber-free bioplastics, along with a more homogeneous surface structure. These findings demonstrate that ramie fiber reinforcement effectively improves the performance of chitosan-based bioplastics.

ARTICLE HISTORY

Received: 02 Dec 2025

Revised: 09 Jan 2026

Accepted: 10 Jan 2026

KEYWORDS

Bioplastics

Chitosan

Ramie Fiber

Mechanical Properties

Water Absorption



Copyright © 2026 Author(s). Published by BRIN Publishing. This article is open access article distributed under the terms and conditions of the [Creative Commons Attribution-ShareAlike 4.0 International License \(CC BY-SA 4.0\)](https://creativecommons.org/licenses/by-sa/4.0/)

INTRODUCTION

Plastic waste remains one of the most persistent environmental challenges globally, due to its largely inorganic nature and resistance to natural decomposition. For instance, plastic waste that is not properly managed can accumulate in soils, rivers, and oceans, causing ecosystem disruption, microplastic formation, and threats to human and animal health [1]. This underscores the urgency for alternative materials that address both waste accumulation and resource sustainability. One promising route is the development of bioplastics: polymeric materials derived from renewable biomass rather than fossil feedstocks. Typically, bioplastics are synthesized from starch or cellulose sources (e.g., cassava, rice, corn) because of their accessibility and renewability. However, a significant technical limitation is that many starch-based bioplastics remain highly hydrophilic and thus suffer from poor water resistance and mechanical stability under moist conditions [2]. Such limitations restrict their utility, especially for packaging or products exposed to humidity or aqueous contact. Therefore, to render bioplastics a genuinely viable alternative to conventional (petroleum-based) plastics, researchers must overcome the water-sensitivity challenge. One strategic avenue is the incorporation of biopolymers with complementary properties, such as chitosan [2], [3].

Chitosan, a deacetylated derivative of chitin, offers many desirable functional features for bioplastic applications: it is biodegradable, non-toxic, has film-forming ability, and importantly exhibits more hydrophobic character compared to pure starch matrices, along with active functional groups (amine and hydroxyl) that can form hydrogen bonds and enhance inter-chain interactions [4]. The addition of chitosan into bioplastic matrices has been shown to improve tensile strength, reduce water uptake, and improve barrier properties, thereby addressing key shortcomings of starch-only bioplastics [2]. Moreover, chitosan's antimicrobial properties can offer additional benefits in packaging applications [4]. While much of the chitosan used in research originates from crustacean shells (crabs, shrimp) as waste streams, research has increasingly shown that fish scales, a widely available underutilised byproduct of the fish processing industry, also contain appreciable chitin/chitosan content [3], [5]. Utilizing fish scale waste thus provides a valuable waste-to-resource pathway, with circular economy implications, especially for maritime and fisheries-rich regions such as Jember.

The extraction process of chitosan from fish scales consists of three main stages: deproteinization, demineralization, and deacetylation [6]. The purpose of the deproteinization process is to remove protein content from the raw material. This stage uses an alkaline solution, typically sodium hydroxide (NaOH). The second stage

is demineralization, which aims to eliminate mineral content. This step employs an acidic solution, commonly hydrochloric acid (HCl). The demineralization process yields chitin, which is then further processed to obtain chitosan through deacetylation. The deacetylation process serves to break the acetyl groups ($-\text{COCH}_3$) in the acetamide groups, converting them into amine groups ($-\text{NH}_2$). This stage is carried out using a highly concentrated NaOH solution [3].

Several previous studies have utilized chitosan as a primary component in bioplastic production. Ayu et al. (2023) [7] reported that increasing chitosan concentration improved the tensile strength and elastic modulus of the bioplastic to 2.7015 MPa and 0.4032 MPa, respectively. Similar findings were observed by Ritonga et al. (2024) [8], who demonstrated that adding crab-shell-derived chitosan to sago pulp-cellulose bioplastics enhanced tensile strength and elastic modulus (1.48 MPa and 12.62 MPa) while also reducing water absorption to 92.68%. In contrast, Motallib et al. (2024) [9] incorporated cellulose nanocrystals into chitosan-gelatin-glycerol bioplastics and found that higher cellulose nanocrystal content increased tensile strength up to 13.93 MPa. Likewise, Sriyana et al. (2023) [10] showed that cellulose fibers from pineapple peel improved the tensile strength of chitosan-glycerol bioplastics to 40.9 MPa. Additional studies [11], [12] also noted that increasing fiber content can reduce water absorption, thereby enhancing the water resistance of bioplastics.

Considering the findings of previous studies regarding the role of chitosan and cellulose-based fibers in enhancing bioplastic performance, this study synthesizes bioplastics using fish-scale-derived chitosan as a form of valorization of underutilized fish-processing waste. The formulation is reinforced with ramie fiber modified using 7% NaOH, which has been reported to yield a cellulose content of 88.643% [13], indicating high crystallinity and strong potential to improve material characteristics. Additionally, citric acid is incorporated as an additive to enhance the bonding of polymer chains between the fibers and chitosan, with the expectation of producing improved mechanical properties, lower water absorption, and a more homogeneous surface structure. The use of citric acid in such formulations has not been previously reported, thus providing a notable novelty in this research. This study further investigates the effect of varying ramie fiber content on the resulting bioplastic characteristics. The synthesized bioplastics are then characterized through tensile testing to determine tensile strength and elastic modulus, water absorption testing to assess moisture resistance, and morphological analysis to examine surface structure. Through these analyses, the influence of ramie fiber addition on the properties of the resulting bioplastics can be comprehensively evaluated.

EXPERIMENTAL METHOD

Materials and Instruments

The main raw materials used in this study were waste fish scales and ramie fiber. The chemicals utilized included sodium hydroxide (NaOH, 99%, Chemical Pure, analytical grade), hydrochloric acid (HCl, 1 N, Smart-Lab), acetic acid (99.85%, Sigma-Aldrich), citric acid (99.5%, Smart-Lab), and distilled water. The instruments used in this research comprised a magnetic stirrer, beakers and volumetric flasks, glass stirrers, filter paper, a pH meter, a 50-mesh sieve, an oven, a blender, glass molds, and aluminum foil.

Chitosan Extraction from Fish Scales

The methods used for chitosan extraction in this study were modified from those in several previous studies [3], [6], [14]. Chitosan extraction from fish scales was carried out through three sequential stages, namely preparation of fish scales, chitin isolation, and chitosan extraction, as illustrated in Figure 1. Clean and dry fish scales were first crushed using a blender or grinder, and the resulting material was sieved through a 50-mesh sieve to obtain fish scale powder with a particle size of approximately ± 0.297 mm. Chitin was then isolated from the powder via deproteinization and demineralization processes. Deproteinization was performed by soaking the fish scale powder in a 3.5% NaOH solution at a ratio of 1:10 (w/v) at 100 °C for 2 hours, followed by filtration and washing with distilled water until a neutral pH was achieved. Demineralization was subsequently conducted by treating the deproteinized material with 1 N HCl at a ratio of 1:6 (w/v) at room temperature for 30 minutes, after which the material was filtered, washed to neutral pH, and dried in an oven at 50 °C for 3 hours to obtain chitin. Finally, chitosan was produced by treating the extracted chitin with a 50% NaOH solution at a 1:10 (w/v) ratio at 100 °C for 1 hour. The resulting product was filtered, washed with distilled water until a neutral pH was reached, and dried at 50 °C for 3 hours to obtain fish scale-derived chitosan.

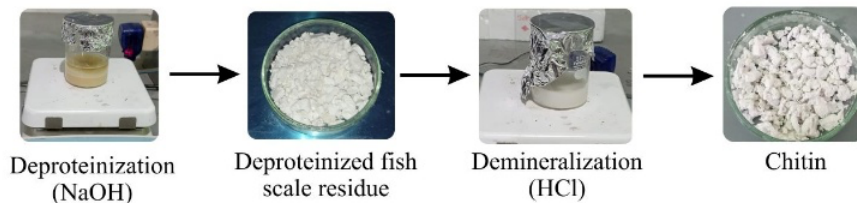
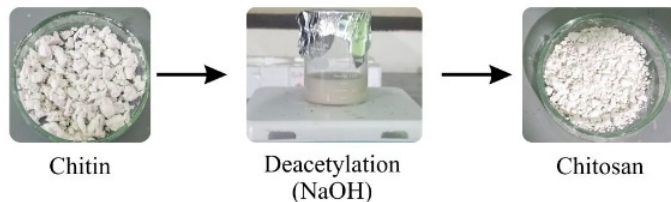
(1) Preparation of fish scales**(2) Chitin isolation****(3) Chitosan extraction**

Figure 1. Schematic illustration of the chitosan extraction process from fish scales.

Ramie Fiber Preparation

Ramie fiber preparation was conducted through an alkali treatment process as schematically illustrated in Figure 2. The treatment of ramie fibers refers to the method used by Jamilah and Sujito (2021) [13] in which the ramie fibers were cut into short lengths of 2–3 mm and then soaked in a 7% NaOH solution. The mixture was stirred using a magnetic stirrer at 70 °C for 5 hours at a speed of 200 rpm. The alkali-treated fibers were then blended and thoroughly washed with acetic acid–acidified water until neutral. Afterward, the fibers were dried under sunlight and subsequently oven-dried at 100 °C for 30 minutes. The dried ramie fibers were then blended again to separate the individual fibers.

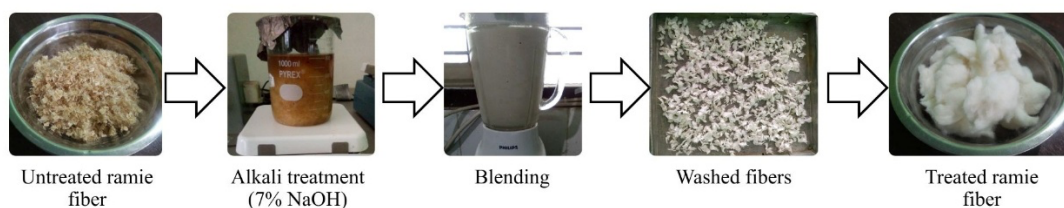


Figure 2. Schematic illustration of ramie fiber modification via alkali treatment (7% NaOH).

Synthesis of Chitosan-Based Bioplastics

Chitosan-based bioplastics were synthesized via a solution casting method with the incorporation of ramie fiber, as schematically illustrated in Figure 3. Bioplastics were synthesized by dissolving 3 grams of chitosan in a 1% acetic acid solution at 50 °C for 4 hours with a stirring speed of 70 rpm. Citric acid (5%) and ramie fiber (15%) were then added to the solution, followed by an additional 1 hour of stirring until a homogeneous mixture was obtained. The bioplastic solution was subsequently poured into molds and dried at 50 °C for 5 hours. This procedure was repeated for different ramie fiber contents of 20%, 25%, and 30% by mass of chitosan. The resulting bioplastic materials were then characterized to determine their tensile strength, elastic modulus, water absorption capacity, and surface morphology. Each formulation was prepared in triplicate to ensure reproducibility.

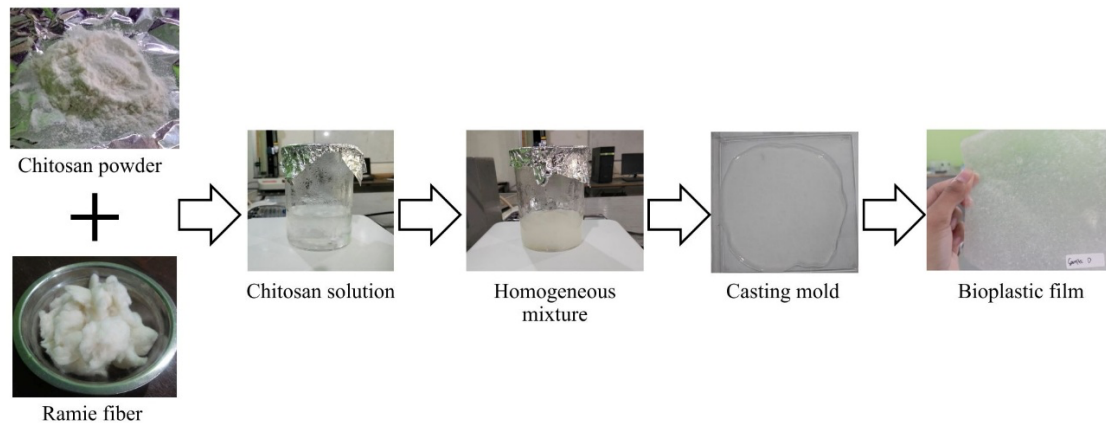


Figure 3. Synthesis of chitosan-based bioplastics with the addition of ramie fiber

Bioplastic Characterization

1. Tensile Test (Tensile Strength and Elastic Modulus)

The tensile test was performed using a Universal Testing Machine (UTM) Hung Ta type HT-2402-10kN. The test results include stress (σ) and strain (ϵ) data, which are plotted into a stress-strain curve to analyze the mechanical properties, including tensile strength and elastic modulus. All tensile measurements were performed in triplicate ($n = 3$) for each formulation, and the results are reported as (mean \pm standard deviation).

2. Water Absorption Test

The water absorption test is used to measure the amount of water absorbed by the bioplastic after immersion in water for 24 hours at room temperature. Before immersion, the bioplastic is dried and weighed (W_0). After immersion, the bioplastic is blotted dry with tissue and weighed again (W_t). The percentage of water absorption is then calculated by comparing the change in mass to the initial mass. Each water absorption test was conducted in triplicate ($n = 3$) to ensure data reliability and reproducibility.

3. Morphological Test (SEM)

Morphological analysis was carried out using a Metkon IMM 902 Scanning Electron Microscope (SEM). Bioplastic sheets were placed in the SEM apparatus, and the scanned surface of the bioplastic was represented in the form of two-dimensional images and then analyzed to determine its surface structure.

4. Statistical Analysis

Statistical analysis was performed using one-way analysis of variance (ANOVA) to evaluate the significance of differences among samples with different ramie fiber contents. A significance level of $p < 0.05$ was adopted to determine statistically significant differences between formulations.

RESULT AND DISCUSSION

The bioplastic material produced in this study was in the form of thin white sheets, which resulted from the addition of ramie fibers during the synthesis process. The synthesized material was then characterized using tensile testing to determine its tensile strength and elastic modulus. In addition, water absorption testing and SEM analysis were conducted to examine the surface structure of the resulting bioplastic. The tensile test results are presented in Table 1.

Table 1. Tensile strength and elastic modulus of bioplastic material with variations in ramie fiber content.

Fiber Content	Tensile Strength (MPa)	Elastic Modulus (MPa)
Sample A (0%)	(17.60 \pm 0.11)	(56.83 \pm 1.69)
Sample B (15%)	(19.68 \pm 0.28)	(36.03 \pm 0.12)
Sample C (20%)	(22.26 \pm 0.55)	(23.25 \pm 1.71)
Sample D (25%)	(39.60 \pm 1.58)	(43.35 \pm 0.89)
Sample E (30%)	(32.69 \pm 0.03)	(27.38 \pm 0.59)

Based on the tensile test results shown in Table 1, one-way ANOVA analysis ($p < 0.05$) confirmed that the increase in tensile strength at 25% ramie fiber content was statistically significant compared to the other

formulations. It is known that the addition of ramie fibers in the synthesis of chitosan-based bioplastic materials can increase the resulting tensile strength. The tensile strength increases as the amount of added fiber increases up to 25%, but decreases when the fiber content exceeds 25%. Meanwhile, the elastic modulus of the material decreases after the addition of ramie fibers. This indicates that ramie fibers are able to reduce the stiffness of chitosan-based bioplastic materials, making them more elastic. This condition becomes more evident when observing the tensile test graph below.

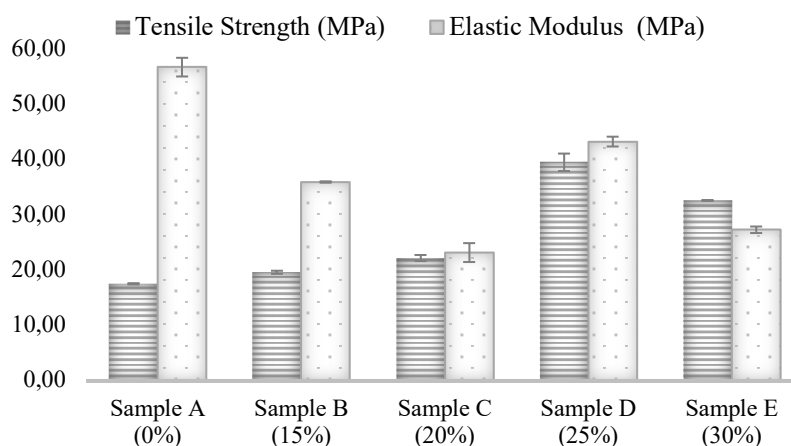


Figure 4. Graph of the relationship between tensile strength and elastic modulus with the addition of ramie fiber content.

Chitosan-based bioplastic material without ramie fiber (sample A) shows low tensile strength (17.60 MPa) but high elastic modulus (56.83 MPa). This pattern indicates that pure chitosan has rigid but brittle characteristics, where its internal structure is densely arranged but lacks flexibility, making it prone to fracture under tensile loading. This behavior is commonly observed in biopolymers dominated by internal hydrogen bonding, as reported by Wardhono et al. (2022) [15], who explained that polymers with extensive hydrogen-bond networks tend to exhibit high elastic modulus but low tensile strength due to limited energy dissipation during deformation. The semi-crystalline nature of pure chitosan further contributes to its high stiffness; however, the absence of reinforcing elements results in low resistance to plastic deformation, leading to premature failure.

When 15% (sample B) and 20% (sample C) ramie fiber were incorporated, the tensile strength increased from 19.68 MPa to 22.26 MPa, indicating that the fibers began to function as reinforcing elements capable of bearing tensile loads. This improvement reflects a more effective stress distribution through the fiber–matrix network, although the interfacial bonding at these fiber fractions is not yet fully optimized. Similar trends have been reported by Lan et al. (2021) [16] and Kamarudin et al. (2022) [17], who observed enhanced tensile strength in natural fiber biocomposites at moderate fiber contents due to fiber bridging mechanisms that delay crack propagation. At these intermediate fiber loadings, the increase in tensile strength is accompanied by a reduction in elastic modulus, which can be attributed to disruptions in the regular packing of the chitosan matrix caused by fiber incorporation without sufficient structural reinforcement. This explains why, at 15–20% fiber content, tensile strength increases while the elastic modulus decreases relative to pure chitosan.

Although the overall trend indicates a reduction in elastic modulus with increasing fiber content, a non-monotonic mechanical behavior is clearly observed at 25% ramie fiber loading (sample D), where both tensile strength and elastic modulus increase to 39.60 MPa and 43.35 MPa, respectively. This paradoxical increase in elastic modulus suggests that the composite system reaches an optimal structural condition at this fiber fraction. At 25% fiber content, ramie fibers are sufficiently well dispersed within the chitosan matrix, and the citric-acid-mediated interactions between chitosan and ramie fibers enhance interfacial adhesion, enabling more efficient stress transfer. In addition, reduced internal porosity and increased polymer network densification contribute to the improved stiffness. Gheribi et al. (2023) [18] similarly reported that intermediate fiber fractions often produce the highest mechanical performance in lignocellulosic biocomposites due to the effective operation of fiber pull-out and crack-bridging mechanisms. Thus, sample D represents the optimum balance between reinforcement efficiency and matrix continuity, resulting in simultaneous enhancement of tensile strength and elastic modulus.

When the ramie fiber content is further increased to 30% (sample E), both tensile strength (32.69 MPa) and elastic modulus (27.38 MPa) decrease, indicating a deterioration in mechanical performance. This decline is

attributed to fiber agglomeration and non-homogeneous fiber distribution, which promote micro-void formation due to insufficient matrix coverage. As reported by Ilyas et al. (2022) [19], excessively high fiber fractions disrupt the balance between matrix availability and fiber surface area, leading to weakened interfacial bonding and inefficient stress transfer. Consequently, excessive fiber loading does not necessarily enhance mechanical properties and may instead compromise the structural integrity of the biocomposite.

Previous studies have consistently demonstrated that the deproteinization process removes protein residues associated with amide I and amide II functional groups, while demineralization effectively eliminates inorganic minerals such as calcium carbonate from fish scale matrices [3], [6]. Subsequent deacetylation converts acetamide groups into free amine groups ($-NH_2$), thereby increasing the polarity and hydrogen bonding capacity of the resulting chitosan [5]. These chemical transformations enhance surface activity and interfacial compatibility, which are critical for effective stress transfer in polymer composite systems. Therefore, although direct FTIR characterization was not conducted in this work, the mechanical performance enhancement and reduced water absorption observed in this study strongly indicate successful chemical modification of the fish scale-derived chitosan, in agreement with well-established literature.

Table 2. Water absorption of bioplastic material with variations in ramie fiber content.

Fiber Content	Water absorption (%)
Sample A (0%)	(213,54 ± 0,66)
Sample B (15%)	(180,13 ± 4,48)
Sample C (20%)	(147,75 ± 0,98)
Sample D (25%)	(121,26 ± 3,37)
Sample E (30%)	(104,96 ± 0,69)

Table 2 presents the water absorption behavior of chitosan-based bioplastics with varying ramie fiber contents. A clear decreasing trend in water absorption is observed with increasing fiber content. The bioplastic without ramie fiber (Sample A) exhibited a water absorption of 213.54%, while the incorporation of 25% and 30% ramie fiber reduced this value to 121.26% and 104.96%, corresponding to reductions of approximately 43% and 51%, respectively. Therefore, the addition of ramie fiber can reduce water absorption by up to ~50%, depending on the fiber content. This reduction indicates decreased porosity and restricted polymer chain mobility, contributing to improved dimensional stability and durability of the bioplastic under humid conditions. These findings are consistent with the review by Ilyas et al. (2022) [19], which reported that natural fiber reinforcement in chitosan biocomposites reduces water uptake through enhanced interfacial interactions and a denser composite structure.

When associated with the tensile test results, there is an indirect relationship between tensile strength and water absorption. At low to moderate ramie fiber content (e.g., 15–25%), tensile strength increases significantly, while water absorption decreases. This indicates that although ramie fibers enhance mechanical properties, they also block water diffusion pathways by filling pore spaces and forming interfacial bonds with chitosan. Previous studies on chitosan–natural fiber composites have also reported a similar pattern, where mechanical enhancement accompanied by reduced absorption occurs because fibers decrease internal porosity and strengthen interfacial bonding [19].

The results of the tensile and water absorption tests can be further supported by SEM imaging of sample D, which is the chitosan-based bioplastic material with 25% ramie fiber addition, as shown in Figure 2.

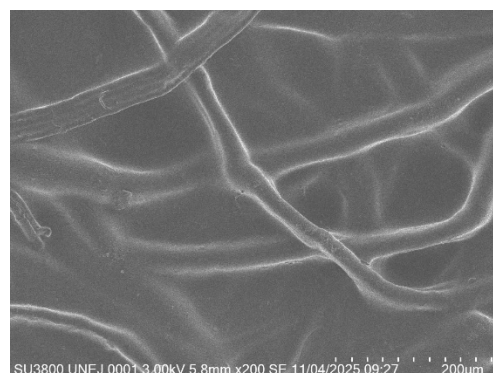


Figure 5. SEM results of the bioplastic sample with 25% ramie fiber (Sample D) at 200× magnification.

The SEM images show that the addition of ramie fiber produces a denser morphological structure, with the fibers being relatively well embedded within the chitosan matrix. This condition indicates the presence of strong physical interactions between the fiber surface and the matrix, thereby reducing voids and microcracks that typically serve as primary pathways for water penetration. The relatively clean and rough fiber surface observed in SEM micrographs indirectly confirms the effectiveness of the alkali treatment and the deproteinization–demineralization processes, which are known to remove surface impurities and expose cellulose microfibrils, thereby improving interfacial bonding with the chitosan matrix. When the internal voids of a bioplastic are minimized, the ability of water to diffuse into the material also decreases significantly. This phenomenon aligns with findings from several studies, which state that increasing the amount of uniformly distributed fiber can enhance structural densification and inhibit water molecule migration in polysaccharide-based biocomposites [20], [21].

In addition to reducing inter-matrix spacing, ramie fibers also act as physical barriers due to their elongated and overlapping orientation. In the SEM images, it can be observed that the fibers form more tortuous pathways, causing water to take longer to penetrate the internal structure. Hydrogen bonding interactions between the –OH groups of ramie and the –NH/–OH groups of chitosan may also enhance compatibility, ultimately producing a more compact material that is harder for water to permeate. This mechanism is consistent with research reports stating that the presence of natural fibers in moderate proportions can improve the relative hydrophobicity of a bioplastic through structural densification and the reduction of water penetration pathways [22], [23].

Overall, the tensile and absorption test results indicate that the addition of ramie fiber not only provides a load-bearing reinforcement mechanism but also alters the physical microstructural properties of the bioplastic. The decrease in absorption suggests densification and more stable interfacial bonding, while the modulus dynamics show that the internal structure changes nonlinearly depending on the fiber fraction. Previous comparative studies, such as on chitosan–cellulose fiber or nanofiller composites, have also reported that modulus and water absorption are strongly influenced by dispersion techniques, fiber orientation, and fiber surface treatment [19]. Therefore, formulation optimization must consider not only improvements in tensile strength but also the balance between stiffness and water resistance so that the resulting material can function effectively in practical applications.

CONCLUSION

This study demonstrates that the utilization of chitosan derived from fish scale waste combined with ramie fiber modified with 7% NaOH can effectively address the common limitations of natural polymer–based bioplastics, which typically exhibit weak mechanical properties and low water resistance. The variation in ramie fiber content significantly influences the properties of the bioplastic, with a fiber content of 25% yielding the optimum performance. At this composition, the bioplastic exhibits a tensile strength of 39.60 MPa, an elastic modulus of 43.35 MPa, and a reduction in water absorption of approximately 43% compared to chitosan-based bioplastic without fiber, accompanied by a denser and more homogeneous microstructure. Overall, the incorporation of ramie fiber is shown to be effective in enhancing the mechanical properties and water resistance of chitosan-based bioplastics, and the 25% fiber composition emerges as the most promising formulation for producing stronger, more stable, and more viable bioplastics as an alternative to conventional plastics.

ACKNOWLEDGEMENT

The researchers would like to express their gratitude to the Materials Physics Laboratory, Faculty of Mathematics and Natural Sciences, University of Jember. This research was funded by the Beginner Lecturer Grant, Research and Community Service Institute, University of Jember, in 2025.

REFERENCES

- [1] P. Rafi and M. Nafa Perkasa, “Dampak Kerusakan Terhadap Lingkungan Yang Disebabkan Oleh Sampah Plastik Berdasarkan Tinjauan Uu No. 18 Tahun 2008,” *Jurnal Multidisiplin Indonesia*, vol. 2, no. 7, pp. 1420–1425, 2023, [Online]. Available: <https://jmi.rivierapublishing.id/index.php/rp>
- [2] S. X. Tan *et al.*, “Characterization and Parametric Study on Mechanical Properties Enhancement in Biodegradable Chitosan-Reinforced Starch-Based Bioplastic Film,” *Polymers (Basel)*, vol. 14, no. 2, Jan. 2022, doi: 10.3390/polym14020278.
- [3] A. A. Ramadhani and N. F. Firdhausi, “Potensi Limbah Sisik Ikan Sebagai Kitosan dalam Pembuatan Bioplastik,” *Jurnal Al-Azhar Indonesia Seri Sains Dan Teknologi*, vol. 6, no. 2, p. 90, Sep. 2021, doi: 10.36722/sst.v6i2.782.
- [4] L. Gallup, M. Trabia, B. O’Toole, and Y. Fahmy, “Predicting the Bending of 3D Printed Hyperelastic Polymer Components,” *Polymers (Basel)*, vol. 15, no. 2, Jan. 2023, doi: 10.3390/polym15020368.
- [5] Y. Ristianingsih, I. A. Hernadin, and D. Timotius, “Chitosan Extraction from Anabas testudineus Scales for Enhancing the Properties of Edible Corn Starch-Based Films: Characterization and Performance Evaluation,” *Makara J Sci*, vol. 29, no. 1, pp. 7–12, Mar. 2025, doi: 10.7454/mss.v29i1.2182.

- [6] R. T. Utami, W. Elvina, D. Pardiansyah, and Y. Yulfiperius, "Pemanfaatan Limbah Sisik Ikan Nila dan Ikan Kakap Merah sebagai Kitosan," *Jurnal Akuakultur Sungai dan Danau*, vol. 8, no. 2, p. 142, Oct. 2023, doi: 10.33087/akuakultur.v8i2.176.
- [7] N. Ayu, E. Jumiati, M. Husnah, J. Fisika, F. Sains, and D. Teknologi, "Analisis Uji Mekanik Bioplastik Berbahan Pati Tepung Sagu-Kitosan Dan Sorbitol," *Agustus*, vol. 8, no. 3, pp. 47–50, 2023.
- [8] H. Ritonga, M. Mashuni, and W. Hardima, "Optimasi Sifat Mekanik Komposit Bioplastik dari Selulosa Ampas Sagu dan Kitosan Cangkang Kepiting," *ALCHEMY Jurnal Penelitian Kimia*, vol. 20, no. 2, p. 190, Sep. 2024, doi: 10.20961/alchemy.20.2.85193.190-197.
- [9] M. A. Mottalib, M. H. Islam, M. C. Dhar, K. Akhtar, and M. A. Goni, "Preparation and Characterization of New Biodegradable Packaging Materials Based on Gelatin Extracted from *Tenualosa ilisha* Fish Scales with Cellulose Nanocrystals," *ACS Omega*, vol. 9, no. 52, pp. 51175–51190, Dec. 2024, doi: 10.1021/acsomega.4c07015.
- [10] H. Yoseph Sriyana, L. Hermawati Rahayu, M. Ema Febriana Politeknik Katolik Mangunwijaya, and J. Sriwijaya No, "Bioplastik Dari Limbah Kulit Buah Nanas Dengan Modifikasi Gliserol Dan Kitosan," *Inovasi Teknik Kimia*, vol. 8, no. 1, pp. 40–44, 2023.
- [11] A. Safitri Agustina, E. Jumrah, and A. Nur Fitriani Abubakar, "Synthesis of Eco-Friendly Bioplastic from Banana Hump Starch and Sugarcane Bagasse Cellulose Filler with Fish Scale Chitosan," *Jurnal Akta Kimia Indonesia*, vol. 16, pp. 44–48, 2023, doi: 10.20956/ica.v1.
- [12] I. Mufida and O. N. Sigiro, "Analisis Biodegradasi Dan Ketahanan Air Pada Plastik Biodegradable Dari Kulit Singkong Dengan Variasi Selulosa Serat Daun Nanas," *Journal of Food Security and Agroindustry*, vol. 2, no. 2, pp. 61–68, Jun. 2024, doi: 10.58184/jfsa.v2i2.357.
- [13] U. L. Jamilah and Sujito, "The Improvement Of Ramie Fiber Properties As Composite Materials Using Alkalization Treatment: NaOH Concentration," *Jurnal Sains Materi Indonesia*, vol. 22, no. 2, pp. 62–70, 2021.
- [14] R. M. Nur and A. Asy'ari, "The Utilitation of Fish Scale Waste as A Chitosan," *Agrikan: Jurnal Agribisnis Perikanan*, vol. 13, no. 2, pp. 269–273, Dec. 2020, doi: 10.29239/j.agrikan.13.2.269-273.
- [15] E. Y. Wardhono *et al.*, "Modification of Physio-Mechanical Properties of Chitosan-Based Films via Physical Treatment Approach," *Polymers (Basel)*, vol. 14, no. 23, Dec. 2022, doi: 10.3390/polym14235216.
- [16] M. Lan, J. Zhou, and M. Xu, "Effect of Fibre Types on the Tensile Behaviour of Engineered Cementitious Composites," *Front Mater*, vol. 8, Nov. 2021, doi: 10.3389/fmats.2021.775188.
- [17] S. H. Kamarudin *et al.*, "A Review on Natural Fiber Reinforced Polymer Composites (NFRPC) for Sustainable Industrial Applications," Sep. 01, 2022, *MDPI*. doi: 10.3390/polym14173698.
- [18] R. Gheribi, Y. Taleb, L. Perrin, C. Segovia, N. Brosse, and S. Desobry, "Development of Chitosan Green Composites Reinforced with Hemp Fibers: Study of Mechanical and Barrier Properties for Packaging Application," *Molecules*, vol. 28, no. 11, Jun. 2023, doi: 10.3390/molecules28114488.
- [19] R. A. Ilyas *et al.*, "Natural-Fiber-Reinforced Chitosan, Chitosan Blends and Their Nanocomposites for Various Advanced Applications," Mar. 01, 2022, *MDPI*. doi: 10.3390/polym14050874.
- [20] S. Chadijah, H. Harianti, A. Febryanti, A. Alif, M. Maulidiyah, and A. A. Umar, "Synthesis of Bioplastics on Rice Straw Cellulose Using Orange Peel Extract, Chitosan, and Sorbitol," *Walisongo Journal of Chemistry*, vol. 5, no. 2, pp. 111–119, Dec. 2022, doi: 10.21580/wjc.v5i2.10090.
- [21] N. J. Ardyansa, A. S. P. Ramadhon, and S. S. Santi, "Effect of Additional Cellulose Bacterial from Nata De Soya and Chitosan in Bioplastic Manufacturing," *Journal of Applied Science, Engineering, Technology, and Education*, vol. 4, no. 2, pp. 202–209, Dec. 2022, doi: 10.35877/454RI.asci1133.
- [22] P. Chen, F. Xie, F. Tang, and T. McNally, "Ionic liquid-plasticised composites of chitosan and hybrid 1D and 2D nanofillers," *Functional Composite Materials*, vol. 2, no. 1, Dec. 2021, doi: 10.1186/s42252-021-00026-0.
- [23] Y. Shi, S. C. Chen, W. T. Xiong, and Y. Z. Wang, "Simultaneous toughening and strengthening of chitin-based composites via tensile-induced orientation and hydrogen bond reconstruction," *Carbohydr Polym*, vol. 275, Jan. 2022, doi: 10.1016/j.carbpol.2021.118713.